

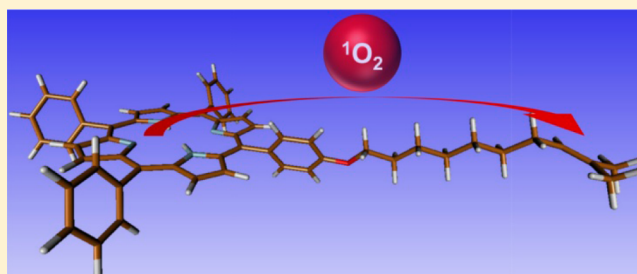
Role of Distance in Singlet Oxygen Applications: A Model System

Matthias Klaper, Werner Fudickar, and Torsten Linker*

Department of Chemistry, University of Potsdam, Karl-Liebknecht-Strasse 24-25, 14476 Golm, Germany

S Supporting Information

ABSTRACT: Herein, we present a model system that allows the investigation of a directed intramolecular singlet oxygen ($^1\text{O}_2$) transfer. Furthermore, we show the influence of singlet oxygen lifetime and diffusion coefficient (D) on the preference of the intramolecular reaction over the intermolecular one in competition experiments. Finally, we demonstrate the distance dependence in quenching experiments, which enables us to draw conclusions about the role of singlet oxygen and $^1\text{O}_2$ carriers in photodynamic therapy.

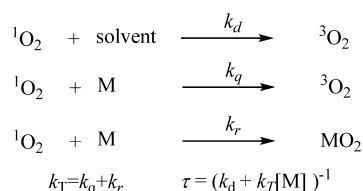


INTRODUCTION

Singlet oxygen ($^1\text{O}_2$)¹ is a very convenient oxidant in organic chemistry and can undergo different reactions, such as Schenck–ene reactions² and $[2 + 2]$ ³- and $[4 + 2]$ -cycloadditions.⁴ It can be generated from its ground state by photosensitization using sensitizers like tetraphenylporphyrin (TPP),⁵ from inorganic sources (H_2O_2),⁶ or with $^1\text{O}_2$ donors like naphthalene endoperoxides.⁷

It has also become very important for the treatment of cancer,⁸ where it is used in photodynamic therapy (PDT).⁹ This technique relies on the precise localization of a sensitizer close to the tumor cells, which are selectively destroyed by light-induced formation of reactive oxygen species (ROS), including $^1\text{O}_2$. One major drawback of PDT is its lack in selectivity toward the target.¹⁰ Owing to its high reactivity, $^1\text{O}_2$ destroys healthy domains when it is either generated or has traveled into these domains.¹¹ Fortunately, the short lifetime of $^1\text{O}_2$ prevents it from traveling larger distances. The lifetime τ is inversely related to rates of deactivation processes arising from physical and chemical interactions with the environment (Scheme 1).

Scheme 1. Modes of Deactivation of $^1\text{O}_2$



The physical quenching by the solvent (k_d) is an unimolecular reaction, whereas chemical reactions (k_r) and the physical deactivation (k_q) with substrates M are bimolecular. The lifetime τ limits the range d where $^1\text{O}_2$ can exist, which correlates with its diffusion coefficient D ($d = \sqrt{2\tau D}$). Using literature data this gives a value of $d = 125$ nm in

water at ambient temperature.¹² The inhomogeneity of a cell is distorting the picture of a uniform diffusion of $^1\text{O}_2$, and the efficiency of transfer of this reactive species depends on the localization of the sensitizer, being either close to (direct transfer) or remote from (indirect transfer) the target (Figure 1).

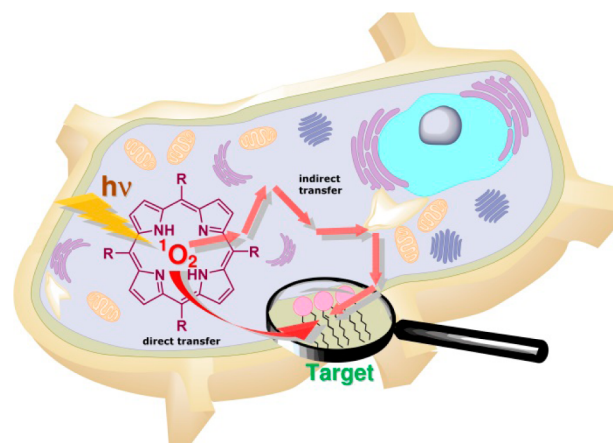


Figure 1. Transfer of $^1\text{O}_2$ from a sensitizer to a target within a cell.

In cells, chemical reactions of $^1\text{O}_2$ with amino acids of proteins, unsaturated lipids, or nucleic acids are effectively reducing its lifetime.¹³ In addition, diffusion coefficients are varying strongly inside the cell. Several strategies were performed in order to determine the effective range d in cells: The group of Ogilby tackled the question by spatially resolving $^1\text{O}_2$ in cells based on the microscopic imaging of the $^1\text{O}_2$ phosphorescence.¹⁴ Surprisingly, the lifetimes measured inside the cell were long, suggesting that chemical quenching processes are negligible. On the other hand, different

Received: February 11, 2016

Published: May 17, 2016

subcellular domains restrict traveling of $^1\text{O}_2$, possibly due to different viscosities inside the cell.^{14b} Other strategies were followed by Moan and Berg, who studied intracellular photodegradation processes of two dyes that could be excited selectively at different wavelengths.¹⁵ Their results revealed that singlet oxygen causes damage at the dye where it is generated rather than at the dye which is not sensitizing. They estimated a travel distance of only 10–20 nm.

A third strategy comprises the investigation of model systems where $^1\text{O}_2$ is transferred within one molecule or within a molecular assembly (intramolecular reaction). Such systems would constitute both the photosensitizer and the $^1\text{O}_2$ target in one entity and would principally resemble modern PDT delivery vehicles, which convey the sensitizer close to the tumor tissue.^{9a}

A single-molecule atomic force microscopy study of a system was performed, where a sensitizer and $^1\text{O}_2$ cleavable linkers were located on a 2D DNA origami.¹⁶ The sensitizer generated $^1\text{O}_2$, which caused chain scission at different positions. For the first time, it was possible to monitor the behavior of $^1\text{O}_2$ in the nanometer range. It was shown that the closer linker was more strongly affected than the further remote one under irradiation of the sensitizer.

To et al. developed an imaging technology where large protein complexes were inserted between a singlet oxygen sensor and generator.¹⁷ Their method allowed confirmation of the topology of protein complexes owing to a distance-dependent $^1\text{O}_2$ transfer.

Very recently, our group investigated such a transfer by using a chemical donor of $^1\text{O}_2$ connected to an acceptor unit.¹⁸ In this study, only one $^1\text{O}_2$ molecule could be donated from the carrier to the acceptor. In competition experiments with a second nonbound acceptor molecule, it was found that the intramolecular transfer prevails, depending on the molecular conformation, the temperature, and the solvent-dependent lifetime of $^1\text{O}_2$. However, the scope of these experiments was limited by the fact that a maximum of only 1 equiv of $^1\text{O}_2$ is available from the donor.

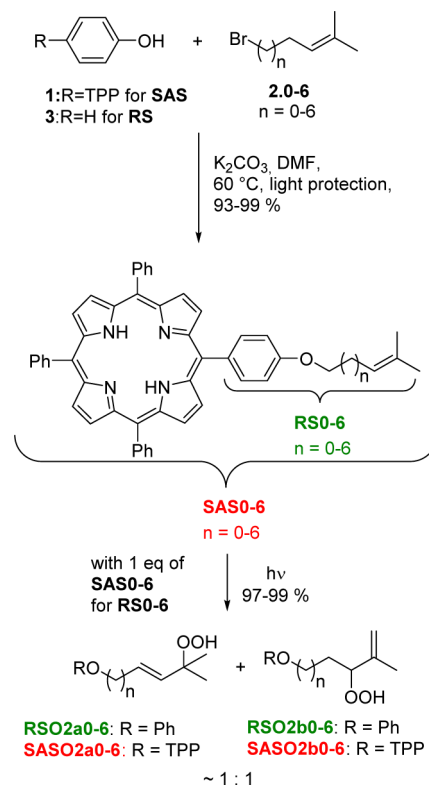
Herein we demonstrate how an intramolecular reaction is controlled in a sensitizer–acceptor system (SAS), where the reactive species can be generated continuously. We will address both the questions of the dependence on the distance and on the surrounding environment, which will reveal important insights into PDT (Figure 1).

RESULTS AND DISCUSSION

We decided to employ a SAS that carries a porphyrin functioning as the $^1\text{O}_2$ -sensitizing unit and an alkene functioning as the $^1\text{O}_2$ acceptor. Both units are connected by alkyl spacers of various chain lengths (SAS n , for $n = 0–6$) separating by varying distances the site where $^1\text{O}_2$ is generated from the site where it is trapped.

For the sensitizing part, we used a hydroxy-substituted tetraphenylporphyrin (TPP), since it has a high $^1\text{O}_2$ quantum yield and is easily accessible.¹⁹ The acceptor is a trimethyl-substituted alkene bound to the termini of spacer units with varying chain lengths ($n = 0–6$). Therefore, porphyrin **1**²⁰ and the bromo compounds **2**²¹ were synthesized according to literature procedures and linked together via a Williamson ether synthesis (Scheme 2 and Supporting Information). The alkene undergoes a Schenck–ene reaction with $^1\text{O}_2$ to give hydroperoxides SASO2a and SASO2b as a mixture of two regioisomers.²² Compared to the donor/acceptor systems,

Scheme 2. Syntheses of Sensitizer–Acceptor and Reference Systems (SAS and RS) and Subsequent Schenck–Ene Reactions to Hydroperoxides



used in our previous work,¹⁸ these photooxygenations can run to full conversion since $^1\text{O}_2$ is generated continuously. In addition to the synthesis of the SAS, it is necessary to have a reference system (RS) that carries only the acceptor unit and the spacer with a phenyl terminus without the sensitizing unit. To avoid different $^1\text{O}_2$ quantum yields, we carried out all photooxygenations of RS with a 1:1 mixture of the corresponding RS/SAS, where $^1\text{O}_2$ is always generated by the porphyrin unit of the SAS linked to an alkyl chain.²³ The RS would resemble the typical situation of an intermolecular reaction, while SAS combines both inter- and intramolecular reactions. Our aim in this study is to control and estimate the contributions of these two reactions in the SAS.

At first, we paid attention to the RS. During irradiation in the presence of ambient atmospheric oxygen of 5×10^{-5} M solutions of both the RS and the corresponding sensitizer²³ in acetonitrile (MeCN), the consumption of starting material was followed by HPLC. The semilogarithmic plot of the concentration versus time gives a straight line that is in accordance with a pseudo-first-order reaction [see figures in the Supporting Information (SI)]. The slope equals the observed rate constant k_{obs} which can be expressed by the following equation:²⁴

$$\ln[A]_t = \ln[A]_0 - (\nu_F k_t / k_d) t = \ln[A]_0 - k_{\text{obs}} t \quad (1)$$

Here, $[A]$ is the concentration of the substrate (RS) and ν_F is the production of $^1\text{O}_2$ (its determination is described in detail in the SI, giving a value of 3.6×10^{-5} M s $^{-1}$ for all following experiments). Note that any other quenching process as mentioned in Scheme 1 is neglected since $k_d \gg k_T[A]$. The bimolecular constants k_t of the seven RS0–6 in MeCN ($k_d = 1.5 \times 10^4$ s $^{-1}$)²⁵ were calculated from eq 1 and are summarized

in Table 1. With exception of the more slowly reacting sterically hindered RS0, the values alternate between 1 and 1.7×10^5

Table 1. Bimolecular Rate Constants k_r of the Schenck–Ene Reactions of the RS in Acetonitrile and Ethanol

entry	RS	n	k_r ($10^4 \text{ M}^{-1} \text{ s}^{-1}$)	
			MeCN	EtOH
1	RS0	0	1.5 ± 0.1	1.5 ± 0.1
2	RS1	1	15.3 ± 0.1	13.9 ± 0.2
3	RS2	2	9.97 ± 0.1	10.4 ± 0.3
4	RS3	3	17.3 ± 0.2	16.1 ± 0.2
5	RS4	4	9.64 ± 0.1	8.3 ± 0.2
6	RS5	5	16.1 ± 0.1	11.3 ± 0.3
7	RS6	6	10.1 ± 0.1	7.4 ± 0.2

$\text{M}^{-1} \text{ s}^{-1}$. Compounds RS1, RS3, and RS5 with an even number of methylene groups between the oxygen atom and the olefinic unit are reacting faster than compounds RS2, RS4, and RS6 with an odd number. Odd–even effects are known to affect molecular properties such as packing, solubility, and phase transitions as well.²⁶

Next, photooxygenations were carried out under the same conditions with the SAS. The slopes of the semilogarithmic plots of SAS0–6 are indeed steeper, as for the corresponding RS0–6 [Figures 2a and S2–S8 (SI), Table 2]. For the SAS the

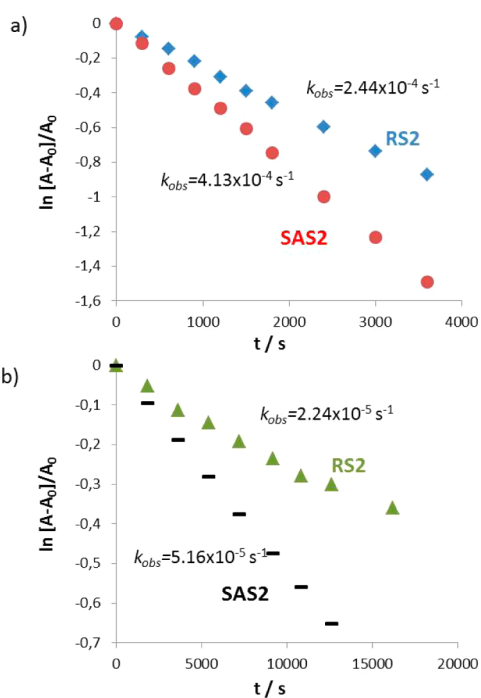


Figure 2. Observed rates of the photooxygenation depicted as semilogarithmic plots: (a) RS2 (blue) and SAS2 (red) in MeCN and (b) RS2 (green) and SAS2 (black) in EtOH.

odd–even effects are preserved at the same degree as for the RS. It is important to note that the comparison between the RS and SAS assumes essentially identical values for k_r , since the reactive centers are identical. To support this postulate, the geometries of SAS0–6 were optimized by DFT calculations (see SI). In such calculations all the SAS are linearly stretched, depicting the reacting olefinic moiety isolated from the pendant macrocycle. Although in solution the alkyl chain should be

more flexible, the above-described odd–even effect speaks for a stretched and not bended chain. We can therefore conclude that electronic and steric influences on these centers are nearly identical. Thus, the observed rate constants k_{obs} for a photooxygenation with a partial contribution of an intramolecular $^1\text{O}_2$ transfer are slightly increased for the SAS. This change is the result of the smaller degree of solvent quenching, since k_d reduces the overall rate k_{obs} .

Consequently, the impact of an intramolecular reaction should become more pronounced when solvent quenching is stronger and k_d is increased. We therefore switched the solvent system to ethanol ($k_d = 7.2 \times 10^4 \text{ s}^{-1}$).²⁵ As expected, the observed rates are strongly reduced as compared to those for the solvent MeCN, but the differences in the slopes between the RS and SAS are increased (Figure 2b, Table 2). Quantitatively, the effect of an intramolecular reaction can be expressed by the ratio of the observed rate constants $k_{\text{SAS}}/k_{\text{RS}}$. From Table 2 it becomes clear that this effect is becoming stronger with increasing solvent quenching.

The biasing of an intramolecular reaction reaches a limit with water as the most quenching solvent ($k_d = 3.2 \times 10^5 \text{ s}^{-1}$).²⁵ However, the solvent water is incompatible with our systems. The domination of the intramolecular reaction of the SAS should become further increased, when the intermolecular reaction of the SAS has to compete with another intermolecular reaction arising from a second substrate that reacts with $^1\text{O}_2$ at a higher rate. Thus, we chose tetramethylethylene (TME), an extremely reactive substrate toward $^1\text{O}_2$ ($k_r = 5.6 \times 10^7 \text{ M}^{-1} \text{ s}^{-1}$).²⁴ Accordingly, the lifetime of $^1\text{O}_2$ is reduced to 1.7 μs , which is less than its lifetime in water (3–5 μs).²⁴ Photooxygenation of TME leads to one single hydroperoxide, which does not undergo further transformations under the present conditions.²⁷ Thus, although organic hydroperoxides are associated with oxidative damage in biologic systems,²⁸ they are well-suited for our model systems.

As described before, irradiation was now carried out in the presence of TME at a concentration of 10^{-2} M . The results of these competition experiments are summarized in Table 3. Here, the intermolecular reaction is suppressed by magnitudes as reflected by the high values of $k_{\text{SAS}}/k_{\text{RS}}$.

The alternating pattern of reactivities found in the two former cases with no TME is reduced but still present. More importantly, the ratio of intra- versus intermolecular reactions ($k_{\text{SAS}}/k_{\text{RS}}$) decreases remarkably with increasing n (Figure 3, Table 3). Thus, we can give evidence for a relationship between the prevalence of an intramolecular reaction and the distance. By means of the calculated structures (see the SI), the distances between the sensitizer and acceptor increase from 12 to 19.5 Å for SAS1 to SAS6. According to Figure 3, the dominance of intramolecular transfer would drop to $k_{\text{SAS}}/k_{\text{RS}} = 1$ at seven or eight methylene groups ($\geq 2 \text{ nm}$). The travel distance of a $^1\text{O}_2$ molecule before quenching under the given conditions is $d = \sqrt{(2k^{-1}D)}$, where k includes all quenching processes and $D = 9.2 \times 10^{-9} \text{ m}^2 \text{ s}^{-1}$. This gives a value of $d = 176 \text{ nm}$. Therefore, the travel distance of $^1\text{O}_2$ is still magnitudes higher than the molecular dimensions of the SAS.

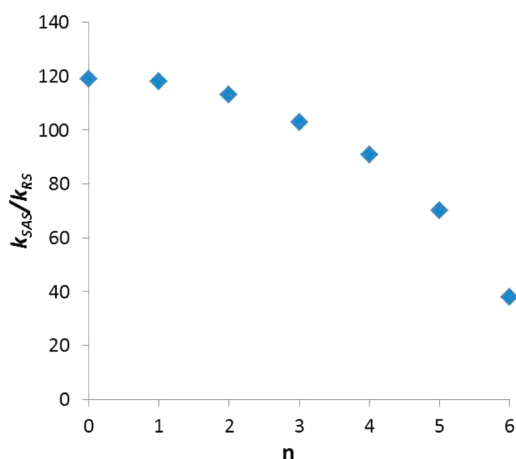
In addition to the revelation of the chain length dependence, we focused on a quantification of the influence of quenchers on biasing an intramolecular reaction in a system such as the SAS as well. Therefore, we first evoke eq 2, which expresses an intermolecular oxygenation of a substrate A in the presence of a second competing substrate A' in excess. This formula should

Table 2. Observed Rate Constants k_{obs} of RS and SAS in Acetonitrile and Ethanol

<i>n</i>	MeCN			EtOH		
	$k_{\text{obs}} (10^{-5} \text{ s}^{-1})$		$k_{\text{SAS}}/k_{\text{RS}}$	$k_{\text{obs}} (10^{-5} \text{ s}^{-1})$		$k_{\text{SAS}}/k_{\text{RS}}$
	RS	SAS		RS	SAS	
0	3.74 ± 0.1	5.11 ± 0.1	1.36	0.37 ± 0.01	0.74 ± 0.01	1.98
1	37.3 ± 0.1	49.8 ± 0.1	1.33	2.48 ± 0.01	6.96 ± 0.03	2.80
2	24.4 ± 0.1	41.3 ± 0.1	1.69	2.24 ± 0.01	5.16 ± 0.01	2.31
3	42.3 ± 0.5	57.8 ± 0.8	1.35	4.17 ± 0.07	7.75 ± 0.06	1.83
4	23.6 ± 0.7	31.1 ± 0.5	1.30	2.78 ± 0.47	4.18 ± 0.02	1.50
5	39.3 ± 0.4	49.9 ± 0.2	1.27	3.77 ± 0.02	5.68 ± 0.03	1.50
6	25.4 ± 0.3	36.8 ± 0.3	1.22	2.48 ± 0.04	3.69 ± 0.02	1.48

Table 3. Observed Rate Constants k_{obs} of RS and SAS in the Presence of TME (200 equiv) in Acetonitrile

entry	<i>n</i>	$k_{\text{obs}} (10^{-5} \text{ s}^{-1})$		$k_{\text{SAS}}/k_{\text{RS}}$
		RS ^a	SAS	
1	0	0.04	4.92 ± 0.01	119
2	1	0.24	28.51 ± 0.01	118
3	2	0.24	27.53 ± 0.02	113
4	3	0.26	26.86 ± 0.4	103
5	4	0.15	13.81 ± 0.02	91
6	5	0.23	16.51 ± 0.01	70
7	6	0.12	4.64 ± 0.05	38

^aError = ±0.01.Figure 3. Preference of intra- over intermolecular reaction ($k_{\text{SAS}}/k_{\text{RS}}$) in the presence of TME as a function of *n*.

be suitable to calculate the rate constants of the photo-oxygenations by knowledge of k_r , k_d , and k'_r .²⁴

$$\begin{aligned} \ln[A]_t &= \ln[A]_0 - (\nu_F k_r / (k_d + k'_r [A'])) t \\ &= \ln[A]_0 - k_{\text{obs}} t \end{aligned} \quad (2)$$

Considering the concentration of $[A']$ as a constant (0.01 M) and using $1.5 \times 10^4 \text{ s}^{-1}$ for k_d , $5.6 \times 10^7 \text{ M}^{-1} \text{ s}^{-1}$ for k'_r (TME), and the k_r values for the RS from Table 1, we obtain k_{obs} ranging between 6.3×10^{-6} and $10.7 \times 10^{-6} \text{ s}^{-1}$. Thus, the expected theoretical values for k_{obs} are higher than the measured values ranging only between 1.2×10^{-6} and $2.6 \times 10^{-6} \text{ s}^{-1}$ (see Table 3). This can be a result from underestimated chemical quenching of TME at this high concentration and from the products generated from the oxygenation of TME. In contrast, if assuming a genuine

intramolecular reaction that is essentially free from any competing reactions and from solvent quenching, the simple eq 3 should become valid.

$$\ln[A]_t = \ln[A]_0 - \nu_F k_r t = \ln[A]_0 - k_{\text{obs}} t \quad (3)$$

The expected theoretical values for k_{obs} would therefore range between 3.6 and 6.1 s^{-1} as compared to the observed rates of the SAS of $(0.4\text{--}2.8) \times 10^{-4} \text{ s}^{-1}$. This strong deviation (factor $\approx 10^4$) shows that quenching processes still occur for the intramolecular reaction under our experimental conditions. Note that k_{obs} calculated from eq 3 deviates, of course, much more strongly for the RS (factor $\approx 10^6$). Even at the shortest distance, SAS1 reacts far too slowly. This may be explained by picturing the environment around a newly born $^1\text{O}_2$ molecule from a SAS. We can consider a hypothetical sphere with the radius d (176 nm as calculated above), centered at the point where $^1\text{O}_2$ was generated. From this point $^1\text{O}_2$ can travel in any direction and can either hit the reactive site or abandon the sphere to be deactivated. However, the reactive site covers only a small sector within the sphere and all other deviating travel directions would cause the loss of $^1\text{O}_2$ (Figure 4). Therefore, geometry-dependent factors become effective, which are also used, for example, for expressing the Förster critical distance.²⁹ It becomes clear that a quantitative intramolecular process would be realized only when the sensitizer is connected with

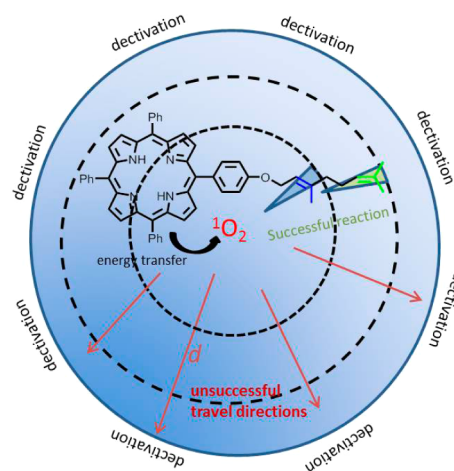


Figure 4. Relationship between the diffusion range d of $^1\text{O}_2$, solvent collisions, and the possibility of an intramolecular reaction. The inner circle depicts the dimensions of a smaller spherical space where collisions occur at closer intramolecular distances (highlighted blue), the circle in the middle depicts a larger sphere for larger distances (highlighted green), and the outermost circle depicts the maximum travel distance of $^1\text{O}_2$ before its deactivation.

multiple acceptors in a 3D dendrimeric structure, covering the entire inner part of the sphere. Thus, the reactions of the SAS proceed more slowly, as expressed in eq 3. This model explains also why the intramolecular prevalence fades out at considerably smaller chain lengths: We may therefore consider spheres with radii r corresponding to the diameters of the SAS. SAS0, for example, would give $V \approx 7 \text{ nm}^3$, and SAS6 would give $V \approx 32 \text{ nm}^3$. Importantly, the volume covered by the reactive centers is the same. Thus, the ratio between the space covered by the reactive space and the total volume drops with r^3 .

From these observations we can draw the following conclusions: An oxygenation reaction where one $^1\text{O}_2$ molecule is attacking exclusively at a site where its generated (either from the same molecule or intermolecularly but within the vicinity of the sensitizer) can be realized only by the use of strong competing quenchers, requiring $k_{\text{quencher}}[A_{\text{quencher}}] \gg k_r$ and a distance between sensitizer and reactive site $\ll \sqrt{(2k_{\text{quencher}}^{-1}D)}$ (see Scheme 1). Fulfillment of these requirements would indeed reduce intermolecular reactions below 1%. On the other hand, the time required for a complete oxidation is increased, which can be predicted using eq 3. For PDT applications, benign quenchers might be available that protect healthy regions from damage by $^1\text{O}_2$. The main challenge remains the accomplishment of the required proximity between the sensitizer and target for a true intramolecular process. The distance dependence found in this work reveals that this proximity is magnitudes smaller than expected.

CONCLUSION

In summary, we synthesized several sensitizer–acceptor systems with different intramolecular distances. The observed rates of their photooxygenations in acetonitrile under continuous irradiation are moderately higher than rates of analogous intermolecular reactions. By using ethanol as solvent, with higher $^1\text{O}_2$ quenching rate, the ratio of intra- versus intermolecular oxidation increases. The most dramatic increase of this ratio by a factor of ≈ 120 , however, is achieved by using an additional chemical $^1\text{O}_2$ quencher. We have presented a quantitative relation of $k_{\text{intra}}/k_{\text{inter}}$ to chemical rate constants, concentrations, and solvent parameters.

In addition, we have shown a strong impact of the distance on this preference in the highly quenching solvent system. For the design of such a sensitizer–acceptor molecule, the distance should not exceed 2 nm. These experimental findings are not conflicting with the much higher predictable travel distance of $^1\text{O}_2$ derived from its lifetime and diffusion coefficient: A $^1\text{O}_2$ molecule generated in the proximity of a reactive site is not inevitably causing a reaction but can travel in other directions. Thus, the sole intramolecular process would require a special 3D molecular architecture, where any travel direction of $^1\text{O}_2$ would lead to a successful encounter. This insight helps one to understand the relations among the diffusion, lifetime, and chemical efficiency of $^1\text{O}_2$ in PDT.

ASSOCIATED CONTENT

Supporting Information

The Supporting Information is available free of charge on the ACS Publications website at DOI: 10.1021/jacs.6b01555.

Experimental procedures and characterization data; sample preparation; determination of k -values, including

plots of c/c_0 versus t ; NMR spectra; and quantum chemical calculations (DOCX)

AUTHOR INFORMATION

Corresponding Author

*linker@uni-potsdam.de

Notes

The authors declare no competing financial interest.

ACKNOWLEDGMENTS

We thank the University of Potsdam for generous financial support. We thank Dr. Heidenreich for assistance in NMR analysis and Dr. Starke for measurement of mass spectra.

REFERENCES

- (1) (a) *Singlet Oxygen*; Frimer, A. A., Ed.; CRC Press: Boca Raton, FL, 1985. (b) *Handbook of Synthetic Photochemistry: Singlet Oxygen as a Reagent in Organic Synthesis*; Greer, A., Zamadar, M., Eds.; Wiley-VCH: Weinheim, Germany, 2010. (c) Ogilby, P. R. *Chem. Soc. Rev.* **2010**, *39*, 3181–3209.
- (2) Adam, W.; Bosio, S. G.; Turro, N. J.; Wolff, B. T. *J. Org. Chem.* **2004**, *69*, 1704–1715.
- (3) Adam, W.; Bosio, S. G.; Turro, N. J. *J. Am. Chem. Soc.* **2002**, *124*, 8814–8815.
- (4) Adam, W.; Prein, M. *Acc. Chem. Res.* **1996**, *29*, 275–283.
- (5) (a) Cló, E.; Snyder, J. W.; Voigt, N. V.; Ogilby, P. R.; Gothelf, K. V. *J. Am. Chem. Soc.* **2006**, *128*, 4200–4201. (b) Frederiksen, P. K.; McIlroy, S. P.; Nielsen, C. B.; Nikolajsen, L.; Skovsen, E.; Jørgensen, M.; Mikkelsen, K. V.; Ogilby, P. R. *J. Am. Chem. Soc.* **2005**, *127*, 255–269. (c) Tørring, T.; Toftgaard, R.; Arnbjerg, J.; Ogilby, P. R.; Gothelf, K. V. *Angew. Chem., Int. Ed.* **2010**, *49*, 7923–7925. (d) McQuade, D. T.; Seeberger, P. H. *J. Org. Chem.* **2013**, *78*, 6384–6389.
- (6) (a) Aubry, J.-M.; Bouttemy, S. *J. Am. Chem. Soc.* **1997**, *119*, 5286–5294. (b) Wahlen, J.; de Vos, D. E.; Groothaert, M. H.; Nardello, V.; Aubry, J.-M.; Alsters, P. L.; Jacobs, P. A. *J. Am. Chem. Soc.* **2005**, *127*, 17166–17167. (c) Pierlot, C.; Nardello, V.; Schrive, J.; Mabille, C.; Barbillat, J.; Sombret, B.; Aubry, J.-M. *J. Org. Chem.* **2002**, *67*, 2418–2423.
- (7) (a) Klaper, M.; Linker, T. *Chem. - Eur. J.* **2015**, *21*, 8569–8577. (b) Martinez, G. R.; Ravanat, J.-L.; Medeiros, M. H. G.; Cadet, J.; Di Mascio, P. *J. Am. Chem. Soc.* **2000**, *122*, 10212–10213. (c) Pierlot, C.; Hajjam, S.; Barthélémy, C.; Aubry, J.-M. *J. Photochem. Photobiol., B* **1996**, *36*, 31–39.
- (8) (a) Cló, E.; Snyder, J. W.; Ogilby, P. R.; Gothelf, K. V. *ChemBioChem* **2007**, *8*, 475–481. (b) Kuimova, M. K.; Yahioglu, G.; Ogilby, P. R. *J. Am. Chem. Soc.* **2009**, *131*, 332–340. (c) Dougherty, T. J.; Gomer, C. J.; Henderson, B. W.; Jori, G.; Kessel, D.; Korbelik, M.; Moan, J.; Peng, Q. *J. Natl. Cancer Inst.* **1998**, *90*, 889–905. (d) Henderson, B. W.; Dougherty, T. J. *Photochem. Photobiol.* **1992**, *55*, 145–157.
- (9) (a) Moor, A. C. E.; Ortel, B.; Hasan, T. *Photodynamic Therapy*; Patrice, M., Ed.; Royal Society of Chemistry: Cambridge, UK, 2003; Chapter 2, pp 19–58. (b) Bonnett, R. *Chem. Soc. Rev.* **1995**, *24*, 19–33. (c) Bartusik, D.; Aebischer, D.; Ghogare, A.; Ghosh, G.; Abramova, I.; Hasan, T.; Greer, A. *Photochem. Photobiol.* **2013**, *89*, 936–941. (d) Tromberg, B.; Kimel, S.; Orenstein, A.; Barker, S.; Hyatt, J.; Nelson, J.; Roberts, W.; Berns, M. *J. Photochem. Photobiol., B* **1990**, *5*, 121–126.
- (10) Orenstein, A.; Kostenich, G.; Roitman, L.; Shechtman, Y.; Kopolovic, Y.; Ehrenberg, B.; Malik, Z. *Br. J. Cancer* **1996**, *73*, 937–944.
- (11) Davies, M. *J. Photochem. Photobiol. Sci.* **2004**, *3*, 17–25. (b) Doleiden, F. H.; Fahrenholtz, S. R.; Lamola, A. A.; Trozzolo, A. M. *Photochem. Photobiol.* **1974**, *20*, 519–521. (c) Sies, H.; Menck, C. F. M. *Mutat. Res., DNAGing: Genet. Instab. Aging* **1992**, *275*, 367–315.

(12) (a) Hatz, S.; Poulsen, L.; Ogilby, P. R. *Photochem. Photobiol.* **2008**, *84*, 1284–1290. (b) Skovsen, E.; Snyder, J. W.; Lambert, J. D. C.; Ogilby, P. R. *J. Phys. Chem. B* **2005**, *109*, 8570–8573.

(13) Redmond, R. W.; Kochevar, I. E. *Photochem. Photobiol.* **2006**, *82*, 1178–1186.

(14) (a) Breitenbach, T.; Kuimova, M. K.; Gbur, P.; Hatz, S.; Schack, N. B.; Pedersen, B. W.; Lambert, J. D. C.; Poulsen, L.; Ogilby, P. R. *Photochem. Photobiol. Sci.* **2009**, *8*, 442–452. (b) Snyder, J. W.; Skovsen, E.; Lambert, J. D. C.; Poulsen, L.; Ogilby, P. R. *Phys. Chem. Chem. Phys.* **2006**, *8*, 4280–4293. (c) Ogilby, P. R. *Photochem. Photobiol. Sci.* **2010**, *9*, 1543–1560. (d) Kuimova, M. K.; Yahioglu, G.; Ogilby, P. R. *J. Am. Chem. Soc.* **2009**, *131*, 332–340.

(15) Moan, J.; Berg, K. *Photochem. Photobiol.* **1991**, *53*, 549–553.

(16) (a) Voigt, N. V.; Tørring, T.; Rotaru, A.; Jacobsen, M. F.; Ravnsbaek, J. B.; Subramani, R.; Mamdouh, W.; Kjems, J.; Mokhir, A.; Besenbacher, F.; Gothelf, K. V. *Nat. Nanotechnol.* **2010**, *5*, 200–203. (b) Helmig, S.; Rotaru, A.; Arian, D.; Kovbasyuk, L.; Arnbjerg, J.; Ogilby, P. R.; Kjems, J.; Mokhir, A.; Besenbacher, F.; Gothelf, K. V. *ACS Nano* **2010**, *4*, 7475–7480. (c) Tørring, T.; Helmig, S.; Ogilby, P. R.; Gothelf, K. V. *Acc. Chem. Res.* **2014**, *47*, 1799–1806.

(17) To, T.-L.; Fadul, M. J.; Shu, X. *Nat. Commun.* **2014**, *5*, 4072.

(18) Klaper, M.; Linker, T. *J. Am. Chem. Soc.* **2015**, *137*, 13744–13747.

(19) Bonnett, R.; McGarvey, D. J.; Harriman, A.; Land, E. J.; Truscott, T. G.; Winfield, U.-J. *Photochem. Photobiol.* **1988**, *48*, 271–276.

(20) Borocci, S.; Marotti, F.; Mancini, G.; Monti, D.; Pastorini, A. *Langmuir* **2001**, *17*, 7198–7203.

(21) (a) Shrestha-Dawadi, P. B.; Lugtenburg, J. *Eur. J. Org. Chem.* **2003**, *2003*, 4654–4663. (b) Mori, K.; Sugai, T.; Maeda, Y.; Okazaki, T.; Noguchi, T.; Naito, H. *Tetrahedron* **1985**, *41*, 5307–5311. (c) Biernacki, W.; Gdula, A. *Synthesis* **1979**, *1979*, 37–38.

(22) (a) Adam, W.; Richter, M. J. *J. Org. Chem.* **1994**, *59*, 3335–3340. (b) Brünker, H.-G.; Adam, W. *J. Am. Chem. Soc.* **1995**, *117*, 3976–3982. (c) Adam, W.; Brünker, H.-G.; Kumar, A. S.; Peters, E.-M.; Peters, K.; Schneider, U.; von Schnering, H. G. *J. Am. Chem. Soc.* **1996**, *118*, 1899–1905.

(23) To ensure consistent $^1\text{O}_2$ quantum yields for all following kinetic experiments, we used the corresponding SAS with the same chain length as sensitizer.

(24) Wilkinson, F.; Helman, W. P.; Ross, A. B. *J. Phys. Chem. Ref. Data* **1995**, *24*, 663.

(25) (a) Ogilby, P. R.; Foote, C. S. *J. Am. Chem. Soc.* **1983**, *105*, 3423–3430. (b) Aubry, J.-M.; Mandard-Cazin, B.; Rougee, M.; Bensasson, R. V. *J. Am. Chem. Soc.* **1995**, *117*, 9159–9164.

(26) Tao, F.; Bernasek, S. L. *Chem. Rev.* **2007**, *107*, 1408–1453.

(27) Dang, H.-S.; Davies, A. G.; Davison, I. G. E.; Schiesser, C. H. *J. Org. Chem.* **1990**, *55*, 1432–1438.

(28) Girotti, A. W. *Lipid Res.* **1998**, *39*, 1529–1542.

(29) Börjesson, K.; Preus, S.; El-Sagheer, A. H.; Brown, T.; Albinsson, B.; Wilhelmsson, L. M. *J. Am. Chem. Soc.* **2009**, *131*, 4288–4293.